
PREDICTING LANDSCAPES FROM ENVIRONMENTAL CONDITIONS USING GENERATIVE NETWORKS

A PREPRINT

Christian Requena-Mesa

Climate Informatics, Institute of Data Science
German Aerospace Center (DLR)
Germany, Jena
crequ@bgc-jena.mpg.de

Markus Reichstein

Max-Planck-Institute for Biogeochemistry
Germany, Jena
mreichstein@bgc-jena.mpg.de

Miguel Mahecha

Max-Planck-Institute for Biogeochemistry
Germany, Jena
mmahecha@bgc-jena.mpg.de

Basil Kraft

Max-Planck-Institute for Biogeochemistry
Germany, Jena
bkraft@bgc-jena.mpg.de

Joachim Denzler

Computer Vision Group
Friedrich-Schiller-Universität
Germany, Jena
joachim.denzler@uni-jena.de

May, 2019

ABSTRACT

Landscapes are meaningful ecological units that strongly depend on the environmental conditions. Such dependencies between landscapes and the environment have been noted since the beginning of Earth sciences and cast into conceptual models describing the interdependencies of climate, geology, vegetation and geomorphology. Here, we ask whether landscapes, as seen from space, can be statistically predicted from pertinent environmental conditions. To this end we adapted a deep learning generative model in order to establish the relationship between the environmental conditions and the view of landscapes from the Sentinel-2 satellite. We trained a conditional generative adversarial network to generate multispectral imagery given a set of climatic, terrain and anthropogenic predictors. The generated imagery of the landscapes share many characteristics with the real one. Results based on landscape patch metrics, indicative of landscape composition and structure, show that the proposed generative model creates landscapes that are more similar to the targets than the baseline models while overall reflectance and vegetation cover are predicted better. We demonstrate that for many purposes the generated landscapes behave as real with immediate application for global change studies. We envision the application of machine learning as a tool to forecast the effects of climate change on the spatial features of landscapes, while we assess its limitations and breaking points.

Accepted as a conference paper at GCPR2019

1 Introduction

The Earth's land surface can be considered a mosaic of landscapes [1]. Landscapes are the material-physical entities that comprise the structures of nature [2]: ecological meaningful units that have a characteristic ordering of elements [3]. Landscapes result from the long-term interaction of abiotic, biotic and anthropogenic processes. The relation

between landscapes and the climatic, geological, and anthropogenic factors is, however, rather conceptual. The totality of interactions and processes that determine the landscapes are impossible to simulate numerically as of today. This fact holds true to such extent that, to the best of our knowledge, landscape imagery prediction is yet to be attempted. We aim to analyze whether the relation between forming factors and landscapes can be mapped with a statistical method. Our goal is to reconstruct the 2D aerial view (multispectral) of the landscapes from a set of 2D environmental conditions. Furthermore, we assess the use of predicting landscapes as a tool for climate change and landscape change studies.

The study of Earth at the landscape scale gained momentum in the last decades benefiting from the use of geographic information systems and the high availability of remotely sensed imagery [4, 5, 6, 7, 8]. Remotely sensed images are a measure of the radiation reflected by the surface. The observed reflections at certain wavelength are information rich snapshots that can be used to diagnose features such as land-cover type, ecosystem spatial structure, vegetation health, water availability or human impact [9, 10, 11]. Predicting the aerial image comes close to predicting the landscapes and their spatial arrangement. From the satellite image, one could derive many high level aspects of the landscapes and ecosystems with existing earth observation tools.

Landscapes are formed by a wide range of components and processes. Factors that determine a landscape can be categorized into largely independent ones (e.g. climate or geology) and dependent ones (e.g. soil or vegetation). A change on the independent factor leads to a change of the dependent ones, for example, changes on abiotic factors generally lead to changes in biotic components (such as shifting position or composition). Previous work to classify the landscapes has determined and ranked the forming factors by importance [12, 13, 3]

$$L = f(C, G, H, S, V, F, U, S). \quad (1)$$

Where L is the Landscape, C is climate, G the geology and geomorphology, H the hydrology, S the soil, V the vegetation, F the fauna, U the land use and S the landscape structure. Developing over the work of [3] we can further reduce the conceptual relationship into the essential independent forming factors

$$L = f(Clim, Geo, AI). \quad (2)$$

Where $Clim$ is the broadened climate, Geo is the lithology and topography and AI are the anthropogenic interventions. As the dependent factors (e.g. soil or vegetation) can be thought of as a function of the independent ones (climate and geology) direct knowledge is not strictly necessary. In addition we broad the definition of climate to encompass all of the meteorological hydrology.

Mechanistic or statistical approaches are scarce, or only address certain aspects (e.g. geomorphological models). Advances in deep learning allow for unsupervised content-based data driven modeling, i.e, neural networks capable of learning the relationship between the spatial features present in the input and output from available data [14]. Ideally, these networks can accommodate the non-linearities that best approximate the functional relation between environmental factors and landscapes generating realistic spatial representations of the landscapes. We aim to demonstrate that it is possible to predict landscapes -as seen from space- that behave as real for hypothetical environmental conditions. We attempt to map the climatic, topographic and anthropogenic factors onto sentinel-2 visible and near-IR bands using a conditional generative adversarial network (cGAN) [15]. We will assess its limitations and usability as a tool for climate change studies. One of the main applications envisioned for the proposed approach is forecasting landscape change under future climate projections.

2 Materials and Methods

Generative adversarial networks (GANs) estimate a generative model via an adversarial process in which two neural networks are trained simultaneously: a generative network G that captures the data distribution and a discriminative network D that estimates the probability of a sample coming from the training set rather than from G . Both networks are co-trained: the network G tries to maximize the probability of D making a mistake while the network D tries to discriminate data generated by G from true samples [16].

In addition, cGANs learn a mapping from input conditions and r probabilistic latent space to the output. Later developed topologies such as the U-Net GAN [14] allow for the input conditions to have two spatial dimensions. With the use of skip-connection between symmetrical convolutional and deconvolutional layers, the conditions do not only determine the features that shall be present in the output, but where those must appear. This is important since, the location of a feature on one of the conditioning variables, e.g., a mountain range in the altitude predictor, must be reflected on the same location on the generated landscape. The mapping from the probabilistic space is relevant since the conditioning variables do not deterministically determine landscapes.

2.1 Problem and notations

To model the problem's uncertainty, we define the ground truth as a probability distribution over the imagery conditioned on the set of environmental conditions C . In training we have access to one sample of the target landscapes for each set of environmental conditions. We train a neural network G to approximate the sought function eq. (2), returning landscapes as seen from space when fed with the environmental conditions

$$G(C, r; \theta) \approx f(Clim, Geo, AI). \quad (3)$$

where θ denotes the network parameter and r is a random variable from which to map the multiple plausible outputs. During test time multiple samples of r could be used to generate different plausible landscapes for the same set of environmental conditions.

2.2 Data

Satellite imagery sensed on April 2017 by Sentinel-2 was matched with 32 environmental predictors representing the *Clim*, *Geo*, and *AI* forming factors for 94,289 locations. The dataset covers 10% of the emerged Earth surface on 1857 blocks of 110×110 Km randomly distributed across the planet. Each location will serve as a single sample with 256×256 pixels, 32 input environmental variables and 4 output multispectral variables. Climatic variables (*Clim*) were represented by a subset of WorldClim v2 [17]. Altitude and lithology (*Geo*) variables, were represented by STRM v4 [18] and GLiM [19]. In addition, we used three of the GlobeLand30's [20] classes as a proxy for anthropogenic large scale interventions (*AI*). All of the environmental variables were resampled to $256 \cdot 256$ pixels to match the resolution of the imagery.

2.3 Experimental Design

Two experiments were designed to asses 1) the ability of the proposed approach to generate landscape imagery and 2) its generalization capability under different spatial block designs to find limitations and describe possible consequences of extrapolation.

Experiment One We first compare five models of different architectural complexity, from a fully connected network to the complex cGAN detailed in the models subsection. For this experiment train and test samples were drawn from a completely randomized pool, 80% of which were used for training and 20% for testing. With this experiment we expect to unveil whether there is a significant performance improvement between the proposed cGAN approach and baseline machine learning methods.

Experiment Two We trained the cGANs of different complexity and the baseline fully connected model under different spatial block designs. Landscapes that are close on the surface of the planet tend to be similar [21]. We split the train and test sets into 3 experimental treatments: a complete randomization of the test and train sets as a baseline; a block design where the test locations must be at least 100 km from the closest training sample; and a third treatment where landscapes in the Americas are predicted by a model trained solely with Asia, Africa and Europe. We expect to be able to measure the negative consequences of overfitting that might arise when extrapolating to locations far from those used for training, and thus, combinations of input conditions never seen during training.

2.3.1 Models

Two cGANs were trained inheriting the architecture of the original pix2pix network [14]: a low complexity one (GAN 1 Gb) with few learnable filters per layer and a high complexity one (GAN 7 Gb), named after the total size of the weights on disk. Alongside with the cGANs a fully connected model lacking spatial context was trained as a baseline. In addition, two handicapped cGAN models were trained in order to compare equally complex models that lack one of the key features. One handicapped cGAN was trained over a modified train set with no spatial features due to random permutation of pixels. It is to expect that this handicapped cGAN will not take advantage of convolutions. The second handicapped cGAN was deprived of the discriminator loss. We would expect it to fail to produce landscapes with sharp photointerpretable features. Further detail of the networks' architectures can be found in the supplementary material.

2.3.2 Analysis

Domain experts can visually determine whether a pair of satellite images resemble the same ecosystem, have a similar climate or have a relatable landscape structures. Experts can identify if a satellite image is realistic or faulty. However, human perception based metrics are costly, time inefficient and prone to bias; therefore, computerized metrics are

needed for the objective comparison of models of results over thousands of samples. The generated landscapes must resemble the target ones, however the generated landscapes do not have to match the targets pixel to pixel. Per pixel error metrics are not adequate since the features of interest on landscapes are of supra-pixel scale, and can appear on different places in the generated imagery.

We tested the generated landscapes by comparing the high level landscape patch metrics [22] to the target landscapes. Landscape metrics are typically used for the objective description of landscape structure. These are central to the study of landscape ecology and biodiversity and habitat analysis [23]. We make use of landscape level patch metrics as a mean to compare landscape composition and structure. While our quantitative analysis is focused on the landscape metrics, it is important to note that predicting these metrics is not the objective of our work. Our objective is to generate landscape images that behave realistic, and we make use of the landscape metrics as a mean of automatizing the evaluation.

In order to compute patch metrics of a landscape, segmentating into landscape units is needed first. These landscape units typically have a semantic meaning such as *forest* or *industrial* and the segmentation process is often carried out by humans. However, in an effort to automatize the analysis, we opted for an unsupervised non-semantic segmentation. The generated and the target satellite imagery was unsupervisedly segmented via K-means clustering using the red, green, blue and near-infrared bands as input variables. The individual pixels were segmented into 20 clusters. A value of $K = 20$ was selected since this is a typical number of land cover units seen in semantically segmented land cover products [24]. For robustness, the analysis was repeated under different landscape segmentations, clustering it in an undersegmentation scenario ($K=8$) and oversegmentation scenario ($K = 60$). A total of 8 K-means were trained using 3,000,000 pixels (3% of total) extracted randomly from 1,500 randomly selected target images (8% of total). Once trained, in a cross-validation fashion, segmentation was performed for 8 randomly selected subsets of size 1,500 sample pairs (each pair consisting of a target and generated landscape).

As landscape metrics are often redundant [25], we selected five representative landscape level metrics of diverse nature based on expert criteria: Shannon diversity index, patch cohesion, connectance, mean fractal dimensionality and effective mesh size. Landscape metrics were computed using FRAGSTATS v4 [26]. Our final evaluation measure is the robust biweight midcorrelation [27] computed as in [28] between generated and target landscapes for patch metrics.

3 Results

3.1 Quantitative Analysis

3.1.1 Experiment One

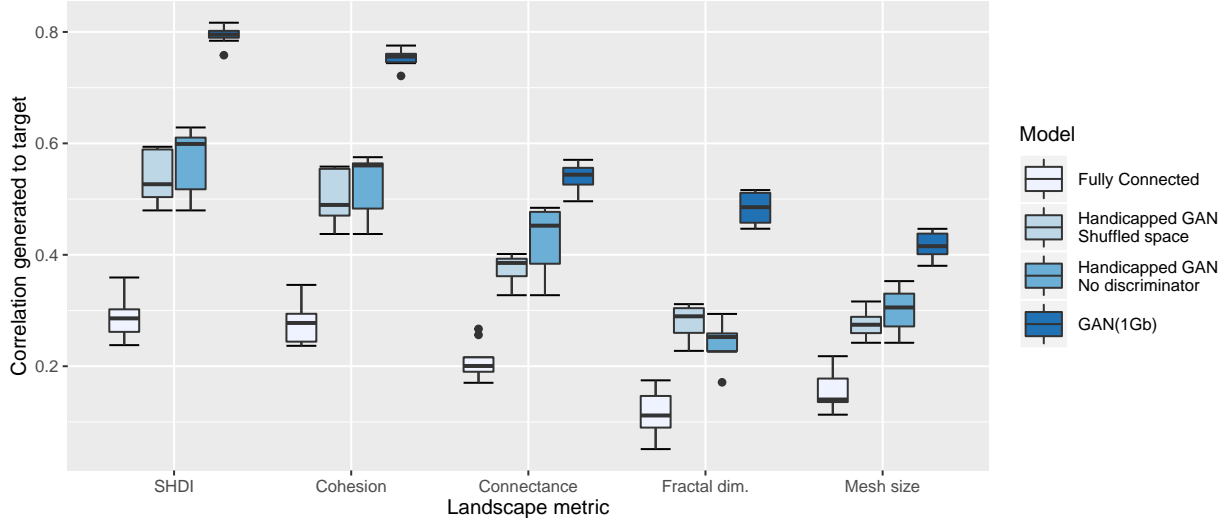


Figure 1: Intermodel comparison (20 landcover units). Correlation between landscape metrics of generated and target landscapes. Shannon diversity index (SHDI), patch cohesion, patch connectance, average patch fractal dimensionality and effective mesh size were computed for both, real landscapes, and landscapes generated given the environmental conditions on the test locations.

Landscapes level metrics' correlation between generated and target landscapes on our first experiment can be seen in fig. 1. The proposed model (GAN 1 Gb) is best at producing landscapes whose patch level metrics resemble the target landscapes. The handicapped models, in spite of having the same number of total weights as the proposed GAN, fail to reproduce the landscape metrics to the same degree. This indicates both, the use of a discriminative training and the capability of mapping spatial features, are key for a high performance. The pixel based 'FC' model is the least capable of generating landscapes whose landscapes composition and structure resemble the targets. Results evidence that for best performance, models that can make explicit use of spatial neighboring on the input features and can generate the landscape as a whole rather than per pixel are needed. In addition, the best performing models are those using a discriminative loss, rather than simple per pixel error metrics. Further evaluation with undersegmented and oversegmented landscapes also lead to similar results (supplementary figures 2 and 3). This indicates that the findings are not dependent on the segmentation process used for calculating the landscape metrics.

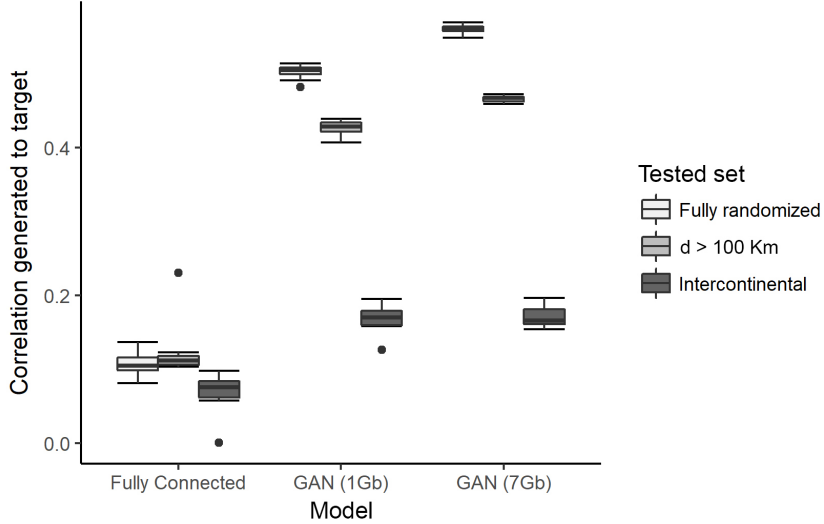


Figure 2: Model generalizability. Correlation between target and generated landscapes' averaged patch metrics. The baseline FC and the two models representing the proposed approach (GAN 1 Gb and GAN 7 Gb) are compared over 3 different test sets. The fully randomized test set is well represented by the training data. The intercontinental set has sample locations on the Americas for models trained with locations on Asia, Europe and Africa. In the intermediate case, the locations are at least 100 Km apart from the closest location used for training.

3.1.2 Experiment Two

On our second experiment we compared our approach and the baseline on a test set that is vaguely represented by the test set due to distance between samples, some extrapolation occurs at prediction time. Landscapes level metrics' correlation generated to target for the proposed model and the baseline can be seen in fig. 2. The proposed GAN models (1 Gb and 7 Gb) outperform the simple baseline method FC. We observe all models suffer some kind of performance decay as location of the testing set samples is further from the train locations. The FC model's performance decays the least with distance, this is to expect of a model that does not suffer from overfitting. The performance of the more complex GAN models decays strongly with extrapolation. While the GAN 7 Gb model slightly outperforms the GAN 1 Gb model on the fully randomized test set and the short distance test, performance becomes similar on the harder intercontinental test. This indicates some level of overfitting to train locations. While the performance decay due to extrapolation is the largest on the GAN 7 Gb, it is to note that it still outperforms the simpler method that does not use spatial context.

3.1.3 Normalized Difference Vegetation Index Prediction

Summary statistics for the prediction of the overall amount of vegetation for all models can be seen in table 1. As NDVI is a simple ratio between different spectral bands, these results can also be understood as the ability of the models to predict overall reflectance.

The simpler models perform close to the GAN models. This effect might be due to the unnecessary of context and spatial features as NDVI is averaged across the image. While by a small margin, the more complex models (GAN 1 Gb

Table 1: Generated to target correlation for the Normalized Difference Vegetation Index

	FC	Spatially shuffled	No discriminator	GAN (1 Gb)	GAN (7 Gb)
Fully randomized	0.934	0.989	0.995	0.991	0.965
$d > 100 \text{ Km}$	0.903			0.980	0.978
Intercontinental	0.716			0.749	0.718

and GAN 7 Gb) outperform the FC baseline models. The higher performance cannot be attributed to the capability of these models to learn spatial features or the discriminative loss, since both handicapped models also outperform the baseline. Therefore, the most plausible cause for the higher performance is the sheer size of the models. Similar to what has been observed for the landscape metrics, the simpler baseline method performance does not decrease as steeply as the GANs when predicting intercontinentally; however, the absolute performance of the GANs is still superior even when extrapolation is done.

3.2 Visual Analysis

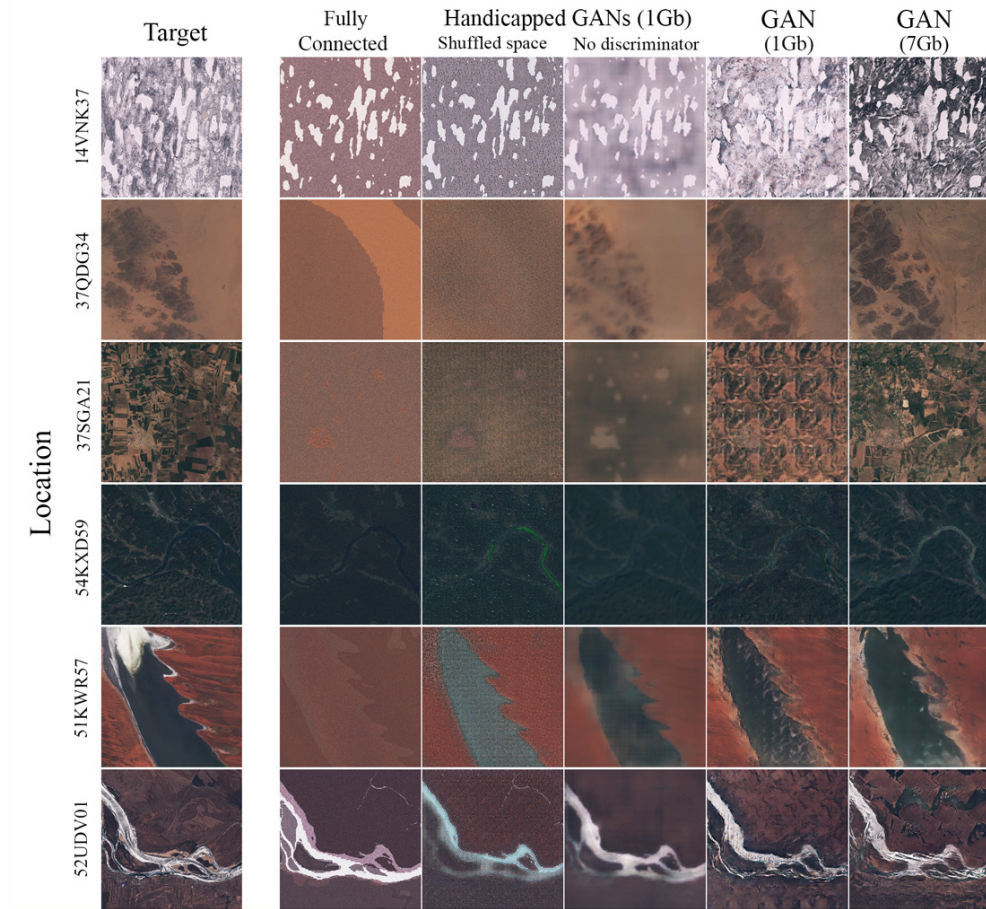


Figure 3: Sample generated landscapes across the tested models. Visible bands on test locations belonging to the fully randomized test set. Model complexity increases from left to right. The six displayed locations were drafted at random.

3.2.1 Experiment One

We first present generated and target landscapes on an ideal scenario where the train dataset represents very well the cases in the test set due to spatial proximity (fig. 3). Landscape reconstructions based on per pixel mapping (FC model) gives overly a close rendition of reflectance across all bands, i.e., colors resemble the target with few exceptions (as seen in sample 14VNK37). Nonetheless, these generated samples lack the characteristic spatial features of landscapes.

This is visible on an agricultural area where the model produces an image that lacks the spatial features of agricultural fields (sample 37SGA21). These samples can hardly be understood as satellite imagery, preventing photointerpretation. Moreover the spatial heterogeneity seen in the output of the fully connected model is directly determined by the spatial heterogeneity of the input condition variables.

The spatially shuffled handicapped GAN faces similar visual problems as the FC model. Although overall colors seem accurate, it still fails to project the expected spatial features of real landscapes as it lacks content-based generation. The outputs are noisier than the fully connected model, possibly due to the spatially shuffling of pixels on the training set and the discriminative loss, i.e., noisy samples, similar to those used for training, had a smaller discriminative loss. The 'No discriminator' handicapped GAN, in contrast, can make use of convolutions but lacks the discriminative training. It generates outputs that contain spatial features loosely resembling those of real landscapes; however, these are smoother. This is an expected artifact when using solely mean squared error as training loss.

GAN models (1 Gb and 7 Gb) generate crisper images. These contain spatial features that humans can recognize as part of landscapes that are not determined by the spatial features in the predictors. The lower complexity model (GAN 1 GB) seems to lack the ability to learn enough spatial features on its generator, and under some circumstances generates mosaicking patterns (as seen in sample 37SGA21) while the model with higher number of convolutional filters per layer (GAN 7 Gb) seems to be able to cope better with spatially homogenous predictors. However, it is still susceptible to generate visually faulty landscapes as seen in sample 52UDV01. Under simple visual inspection, the proposed models (GAN 1 Gb and 7 Gb) seem to be the ones generating imagery that is most readily accessible to photointerpretation.

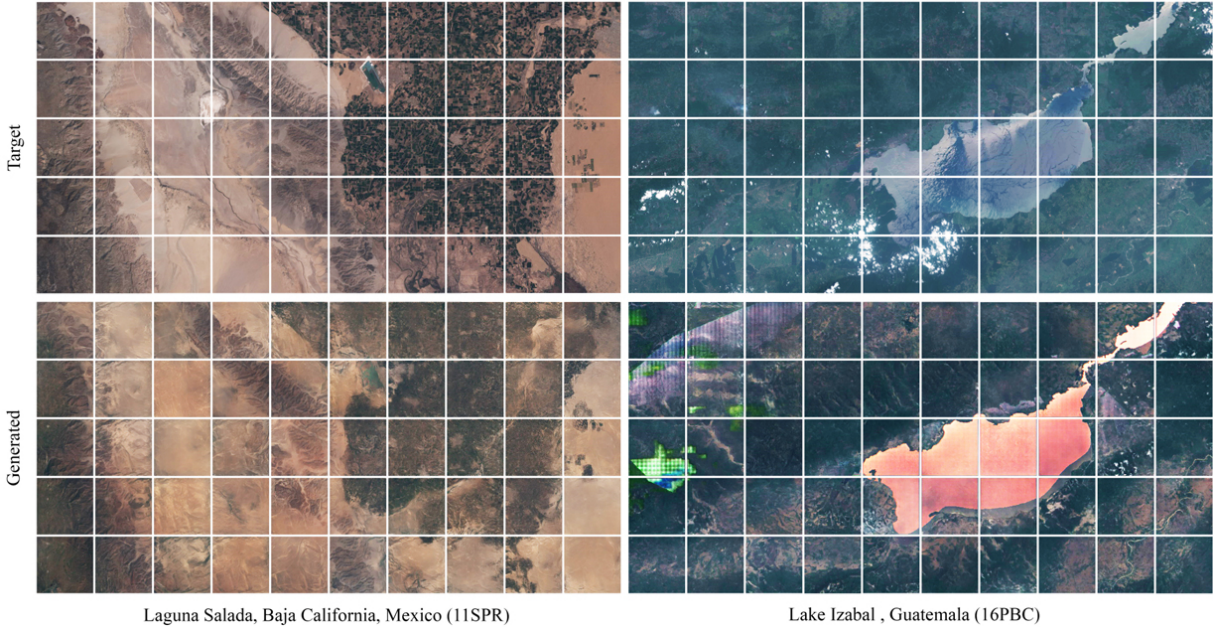


Figure 4: Generated test samples by a GAN (7 Gb) for the intercontinental test set. The model used to generate the landscapes was trained solely with imagery of Europe, Africa and Asia, however the input conditions given to generate the images occur in the Americas. Each square image was generated independently and mosaicked to display a larger area.

3.2.2 Experiment Two

We trained the models with samples from Europe, Africa and Asia to later generate samples for environmental conditions occurring on the Americas. Samples from a good and a bad case were re-mosaicked for display on fig. 4. While Laguna Salada landscape does not show large scale artifacts, Lake Izabal landscape displays colors and features that are not possible on a real landscape, such as a red water lake or bright green vegetation, as well as, repetitive patterns.

4 Discussion

We tackled the prediction of landscapes as seen from space by linking reflectance and environmental conditions with a generative neural network. The proposed approach is able to generate photointerpretable satellite imagery. This is the

first time it has been achieved. We unveiled that both, a discriminative loss and spatial context are key for the good performance of the model. In addition, spatial extrapolation to new areas is possible to some extent.

Nonetheless, there are artifacts of different nature in the generated imagery, especially for the test locations that are far from the train locations. We hypothesize these artifacts could be caused by a combination of the following reasons: 1) the deep dreamy appearance might be a negative consequence of the discriminative loss; 2) the model might be overfitting our training set; 3) the input environmental conditions were never seen during training; 4) the processes involved in creating landscapes are not identical in different parts of the planet. These results highlight the importance, when using this approach as a tool, of training the model with a set of samples that is as relevant as possible to the problem to be solved.

4.1 Predicting Landscapes as a Tool

Predicting landscapes could become an important tool for the study of ecological change at the landscape scale. However, further effort is needed as the proposed approach is by no means exempt of flaws and projecting future climate scenarios is only valid under rigorous assumptions.

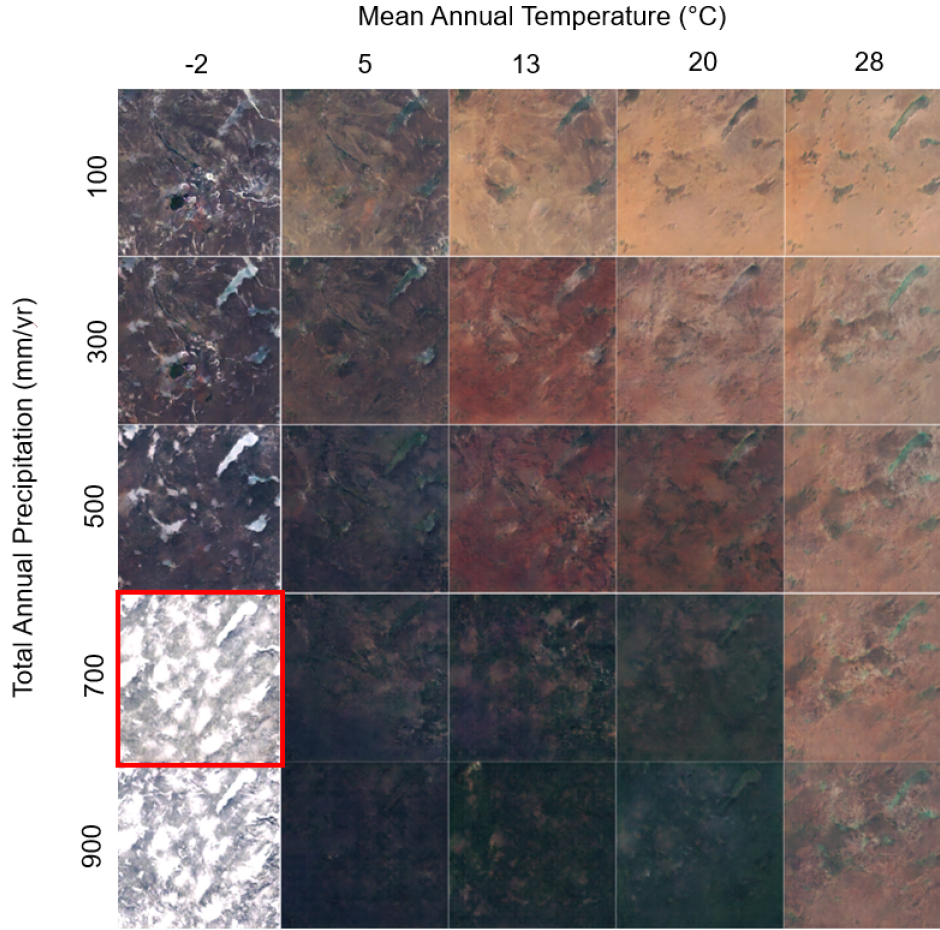


Figure 5: Satellite imagery generated for hypothetical environmental conditions. Annual precipitation and temperature were modified over a real location in northern Canada ($56^{\circ}48'37''\text{N}$, $106^{\circ}32'36''\text{W}$) in order to display the ability of the model to create novel landscapes for hypothetical climate scenarios. The real landscape is marked in red.

One of the main applications envisioned for the proposed approach is forecasting landscape change under future climate projections. In fig. 5 a sample test location is altered both, annual precipitation and mean annual temperature, in order to display the capability of the model to reimagine landscapes under different environments. Validating the landscapes depicted in fig. 5 is not possible; however, the increase of vegetation cover and the desertification as temperature and precipitation varies is consistent with our expectation. While, made up predictors generate landscapes never seen and

thus, difficult to validate, we have tested against predictors found in real world mid distance (more than 100 Km away) and long distance (intercontinentally) and the landscapes generated do resemble the real landscapes to a high extent.

There are, however, limitations to be taken into account before using these models for projecting future landscapes. Our approach, in its current status, does not account for the temporal processes; instead, if we were to predict future scenarios we would be assuming space for time, e.g., sometime warmer in the future must look like somewhere warmer today. However, this assumption only holds if you allow ample time for the landscape to achieve a new steady state after the intervention. When climatic conditions change rapidly, landscape change lags behind, and thus, modelling the landscapes inertia and temporal dynamics is necessary. Also with global change other factors such as CO_2 change, having an important effect on vegetation that a static model cannot predict. In addition, in order to generate landscapes for hypothetical environmental conditions, we assume that the system is currently in steady state. However, we know that current climate is trending [29]. Therefore, since our train set landscapes are not in equilibrium with the environmental conditions, our ability to predict landscapes for the future climates is further detrimented. The data driven modelling of the evolution of landscapes over time given the environmental conditions might serve as a fix to most of the flaws previously mentioned.

Although landscapes are shaped by past environmental conditions, for simplicity, we have assumed that present day conditions are sufficient. As a matter of fact, present day conditions may serve as a proxy for past climatic conditions. While this is true for orbital processes, it is not for the tectonic processes or glaciations [30].

Predicting the landscape patch composition and structure is not the only use that can be made of the imagery. The generated satellite imagery can be potentially used across many disciplines. There are many available tools for different scientific purposes that make use of satellite imagery to gather information. It is unknown whether the quality of the generated imagery is sufficient for these tools to work seamlessly and will require specific testing for the different use cases.

4.2 Problems

Predicting landscapes as seen from space is an ill-posed problem. Landscapes are stochastic and chaotic systems and their evolution is conditioned on an unknown initial state. For added difficulty, landscapes have become dependent on complex societal and economical systems that are hard to predict as well. We cannot expect our method or any future method to predict landscapes without flaws and compromises.

We have experienced technical problems. We observe mode collapse. The GAN network we use [14] does not explicitly model the uncertainty since no r probabilistic space is used during the generative process. Instead, it does so in a weak manner by having an active dropout during test time as explained in [14]. When fed the same set of environmental conditions, the network outputs nearly identical landscapes. Later developed network architectures, such as those using an implicit probabilistic space and making use of Wasserstein distance during training might mitigate the observed mode collapse. Predicting the full set of landscapes that are plausible for a set of environmental conditions is key in order to have a measure of uncertainty over our prediction.

4.3 Future Work

Predicting imagery of landscapes is a valid line of research; furthermore, future improvements in deep learning must be expected making the prediction of satellite imagery more feasible.

- Modeling explicitly landscape evolution over time could greatly benefit the usability as a tool.
- Improve landscape comparison metrics: comparing generated and target landscapes is not trivial. Learned perceptual similarity based metrics [31] might be a faster and better option than landscape metrics.
- Extract knowledge from the network. Exploring the latent space might give us new insight to the importance of the forming factors, the relation between them and help clustering the surface of Earth landscape-wise.
- Build a working stochastic generator. Generate the multiple plausible landscapes that can arise from each set of environmental factors.

5 Summary and Conclusion

We have tackled the prediction of landscapes as seen from space by approximating the conceptual model with a generative neural network. The proposed approach demonstrates that a minimum set of environmental conditions is enough to predict landscapes. Our trained model allows to generate close to realistic landscapes for hypothetical

environmental scenarios that have some degree of photointerpretability. To the best of our knowledge, this is the first time that environmental predictors are used to infer the aerial view of landscapes.

The predicted images of the landscapes have spatial features that are not dictated by the predictors, but introduced by the generative model. These spatial features add for the interpretability as evidenced by our experiments (fig. 3), making the generated landscapes behave closer to the real ones as evidenced by patch level landscape metrics fig. 1). We contribute our dataset covering 10% of the emerged surface of Earth and matched with the pertinent 32 environmental predictors (detailed in Supplementary Material) for further development. We believe this is an important step for the data-driven modeling and forecasting of Earth surface.

The use of a discriminative loss and spatial context is crucial in order to generate landscape images susceptible to photointerpretation. We see how a minimum set of with only present day environmental conditions provide enough information to infer the aerial view of a landscape. We demonstrate for the first time that landscapes, as seen from space, can be predicted by pertinent environmental conditions, opening a new data-driven way to study the landscape evolution.

References

- [1] Richard TT Forman. Some general principles of landscape and regional ecology. *Landscape ecology*, 10(3):133–142, 1995.
- [2] Günter Haase and H Richter. Current trends in landscape research. *GeoJournal*, 7(2):107–119, 1983.
- [3] Caspar A Mücher, Jan A Klijn, Dirk M Wascher, and Joop HJ Schaminée. A new european landscape classification (lanmap): A transparent, flexible and user-oriented methodology to distinguish landscapes. *Ecological indicators*, 10(1):87–103, 2010.
- [4] SE Franklin, EE Dickson, MJ Hansen, DR Farr, and LM Moskal. Quantification of landscape change from satellite remote sensing. *The Forestry Chronicle*, 76(6):877–886, 2000.
- [5] Geoff Groom, CA Mücher, Margaret Ihse, and Thomas Wrbka. Remote sensing in landscape ecology: experiences and perspectives in a european context. *Landscape Ecology*, 21(3):391–408, 2006.
- [6] Jeremy T Kerr and Marsha Ostrovsky. From space to species: ecological applications for remote sensing. *Trends in ecology & evolution*, 18(6):299–305, 2003.
- [7] Adrian C Newton, Ross A Hill, Cristian Echeverría, Duncan Golicher, Jose M Rey Benayas, Luis Cayuela, and Shelley A Hinsley. Remote sensing and the future of landscape ecology. *Progress in Physical Geography*, 33(4):528–546, 2009.
- [8] MA Simmons, VI Cullinan, and JM Thomas. Satellite imagery as a tool to evaluate ecological scale. *Landscape Ecology*, 7(2):77–85, 1992.
- [9] Vittorio E Brando and Arnold G Dekker. Satellite hyperspectral remote sensing for estimating estuarine and coastal water quality. *IEEE transactions on geoscience and remote sensing*, 41(6):1378–1387, 2003.
- [10] Stephan Getzin, Kerstin Wiegand, and Ingo Schöning. Assessing biodiversity in forests using very high-resolution images and unmanned aerial vehicles. *Methods in Ecology and Evolution*, 3(2):397–404, 2012.
- [11] J Otterman. Anthropogenic impact on the albedo of the earth. *Climatic Change*, 1(2):137–155, 1977.
- [12] Robert Gerald Henry Bunce, CJ Barr, RT Clarke, DC Howard, and AMJ Lane. Land classification for strategic ecological survey. *Journal of environmental management*, 47(1):37–60, 1996.
- [13] JA Klijn. Hierarchical concepts in landscape ecology and its underlying disciplines. *DLO winand staring centre report*, 100, 1995.
- [14] Phillip Isola, Jun-Yan Zhu, Tinghui Zhou, and Alexei A Efros. Image-to-image translation with conditional adversarial networks. *arXiv preprint arXiv:1703.10021*, 2017.
- [15] Mehdi Mirza and Simon Osindero. Conditional generative adversarial nets. *arXiv preprint arXiv:1411.1784*, 2014.
- [16] Ian Goodfellow, Jean Pouget-Abadie, Mehdi Mirza, Bing Xu, David Warde-Farley, Sherjil Ozair, Aaron Courville, and Yoshua Bengio. Generative adversarial nets. In *Advances in neural information processing systems*, pages 2672–2680, 2014.
- [17] R J Hijmans, S Cameron, J Parra, P Jones, A Jarvis, and K Richardson. WorldClim-Global Climate Data. Free Climate Data for Ecological Modeling and GIS, 2015.

- [18] Andy Jarvis, Hannes Isaak Reuter, Andrew Nelson, and Edward Guevara. Hole-filled srtm for the globe version 4. 2008.
- [19] Jens Hartmann and Nils Moosdorf. The new global lithological map database GLiM: A representation of rock properties at the Earth surface. *Geochemistry, Geophysics, Geosystems*, 13(12), 2012.
- [20] Chen Jun, Yifang Ban, and Songnian Li. China: Open access to Earth land-cover map. *Nature*, 514(7523):434, 2014.
- [21] David R Roberts, Volker Bahn, Simone Ciuti, Mark S Boyce, Jane Elith, Gurutzeta Guillera-Arroita, Severin Hauenstein, José J Lahoz-Monfort, Boris Schröder, Wilfried Thuiller, et al. Cross-validation strategies for data with temporal, spatial, hierarchical, or phylogenetic structure. *Ecography*, 40(8):913–929, 2017.
- [22] Jeffrey A Cardille and Monica G Turner. Understanding landscape metrics. In *Learning landscape ecology*, pages 45–63. Springer, 2017.
- [23] Evelin Uuemaa, Marc Antrop, Jüri Roosaare, Riho Marja, and Ülo Mander. Landscape metrics and indices: an overview of their use in landscape research. *Living reviews in landscape research*, 3(1):1–28, 2009.
- [24] Jefferson Fox and John B Vogler. Land-use and land-cover change in montane mainland southeast asia. *Environmental Management*, 36(3):394–403, 2005.
- [25] Samuel A Cushman, Kevin McGarigal, and Maile C Neel. Parsimony in landscape metrics: strength, universality, and consistency. *Ecological indicators*, 8(5):691–703, 2008.
- [26] K McGarigal, S A Cushman, M C Neel, and E Ene. FRAGSTATS v4: Spatial Pattern Analysis Program for Categorical and Continuous Maps. University of Massachusetts, Amherst, MA. URL <http://www.umass.edu/landeco/research/fragstats/fragstats.html>, (2007), 2012.
- [27] Rand R Wilcox. Robust generalizations of classical test reliability and cronbach’s alpha. *British Journal of Mathematical and Statistical Psychology*, 45(2):239–254, 1992.
- [28] Peter Langfelder and Steve Horvath. Fast r functions for robust correlations and hierarchical clustering. *Journal of statistical software*, 46(11), 2012.
- [29] Myles R Allen, Vicente R Barros, John Broome, Wolfgang Cramer, Renate Christ, John A Church, Leon Clarke, Qin Dahe, Purnamita Dasgupta, Navroz K Dubash, et al. Ipcc fifth assessment synthesis report-climate change 2014 synthesis report. 2014.
- [30] James Zachos, Mark Pagani, Lisa Sloan, Ellen Thomas, and Katharina Billups. Trends, rhythms, and aberrations in global climate 65 ma to present. *science*, 292(5517):686–693, 2001.
- [31] Richard Zhang, Phillip Isola, Alexei A Efros, Eli Shechtman, and Oliver Wang. The unreasonable effectiveness of deep features as a perceptual metric. In *Proceedings of the IEEE Conference on Computer Vision and Pattern Recognition*, pages 586–595, 2018.

6 Supplementary Material

6.1 Dataset

The sample satellite imagery was sensed by the Sentinel-2 and dated in April 2017 for random locations across the globe. We collected 1,857 level-1C tiles of $110 \times 110 \text{ km}^2$ each from latitude 56°S to 60°N with less than 20% cloud cover. Each tile was subdivided into 10×10 cells, each cell is treated as a single sample of $11 \times 11 \text{ km}$. The samples missing data total or partially were discarded. A total of 94,289 samples were obtained and resampled to $256 \cdot 256$ pixels, resulting in 43 m/pix resolution. Only blue, green, red and near-infrared spectral bands were considered.

Environmental predictors were collected and matched to each sample location. Climatic variables (*Clim*) were represented by a subset of WorldClim v2 [17]: annual precipitation, mean annual temperature, precipitation of the wettest month, precipitation seasonality, precipitation of the driest month, maximum annual temperature, minimum annual temperature, mean diurnal range, isothermality, temperature seasonality and annual temperature range. Altitude and lithology (*Geo*) variables, were represented by STRM v4 [18] and GLiM [19] of which only the 18 high level lithological classes were used as predictors. In addition, we used three of the GlobeLand30’s [20] classes: agriculture, artificial and urban, and waterbody, as a proxy for anthropogenic large scale interventions (*AI*). All of the environmental variables were resampled to $256 \cdot 256$ (43 m/pix) to match the resolution of the satellite imagery. It is to note that climatic variables are known to a coarser spatial resolution than desired (1 km/pix).

The area of Earth covered by the samples is 22.38 Million km^2 . Our dataset accounts approximately for 10% of the emerged surface of the Earth. Although good in size, the dataset is not perfect; the representation of biomes

is unbalanced: due to the low cloud cover requisite deserts are overrepresented; some of the input environmental conditions are highly collinear; some samples cover mainly sea surface as some satellite intakes might be close to coastal areas; and there are a few areas of the planet where one or several predictors have missing values.

6.2 Models

Two cGANs were trained, a low complexity one (fewer learnable filters per layer) and a high complexity one, named after the total size of the weights on disk. The small model has 57 million weights (accounting for generator and discriminator) named ‘GAN 1 Gb’ the high complexity model has 348 million weights, the ‘7 Gb’ model.

The ‘1 Gb’ GAN (low complexity) consists of a generator with symmetric encoder and decoder, skip connections (U-net) and a convolutional discriminator. It has 7 layers of two-dimensional convolutions with the following number of learnable 4×4 filters: $64 - 128 - 256 - 512 - 512 - 512 - 512$ and exactly symmetrical deconvolutional decoder with 0.5 dropout on the last three layers. Leaky relu activation and batch normalization is used at every convolutional step on the encoder. Relu activation and batch normalization at every deconvolutional step on the decoder except for the output layer that uses hyperbolic tangent activation. The discriminator consists of 5 convolutional layers with $64 - 128 - 256 - 512 - 1$ filters of size 4×4 , leaky relu activation and batch normalization at every step and sigmoid activation on the output layer. The ‘7 Gb’ (high complexity) GAN model only differs on the number of filters on the generator ($160 - 320 - 640 - 1280 - 1280 - 1280 - 1280$) and discriminator ($160 - 320 - 640 - 1280 - 1$).

Alongside with the cGANs, a fully connected model lacking spatial context was trained as a baseline. The fully connected network takes the value of the environmental variables as scalar inputs (32 input variables) and performs regression on the reflectance value for each spectral band (RGB and near infrared). The network has three fully connected hidden layers (64, 256, 364) using hyperbolic tangent activation for the hidden layers and a linear activation for the last layer. The fully connected network totals 113,000 parameters. In addition, two handicapped cGAN models were trained in order to compare the cGANs to other models with the same complexity but lacking one of the key features. On one hand, a handicapped cGAN was trained over a modified train set with no spatial features due to random permutation of pixels. It is to expect that this handicapped cGAN will not take advantage of convolutions, since there are no spatial relations on the training set. On the other hand, the second handicapped cGAN was deprived of the discriminator loss, i.e., it was trained solely based on mean squared error. In this case we would expect it to fail to produce landscapes with sharp photointerpretable features.

6.3 Supporting Figures

Landscapes are segmented into landcover units before calculating patch level metrics. The following image depicts several landscape images together with their unsupervised segmentation ($K=20$)

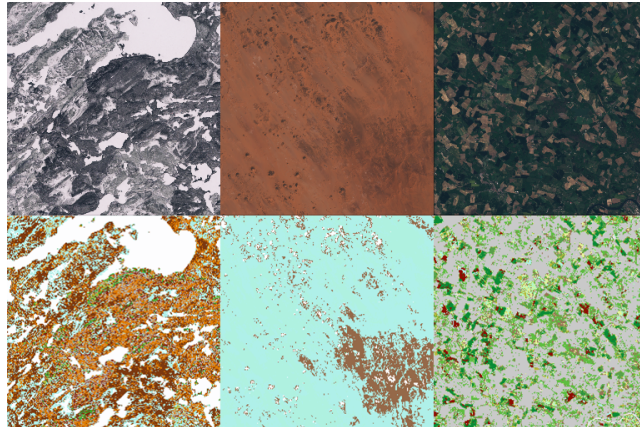


Figure 6: **Landscape segmentation** Example landscapes and their unsupervised pixel-wise segmentation ($k = 20$).

Further replicates of the main quantitative analysis for undersegmented scenario ($K=8$) and oversegmented scenario ($K=60$) are displayed next.

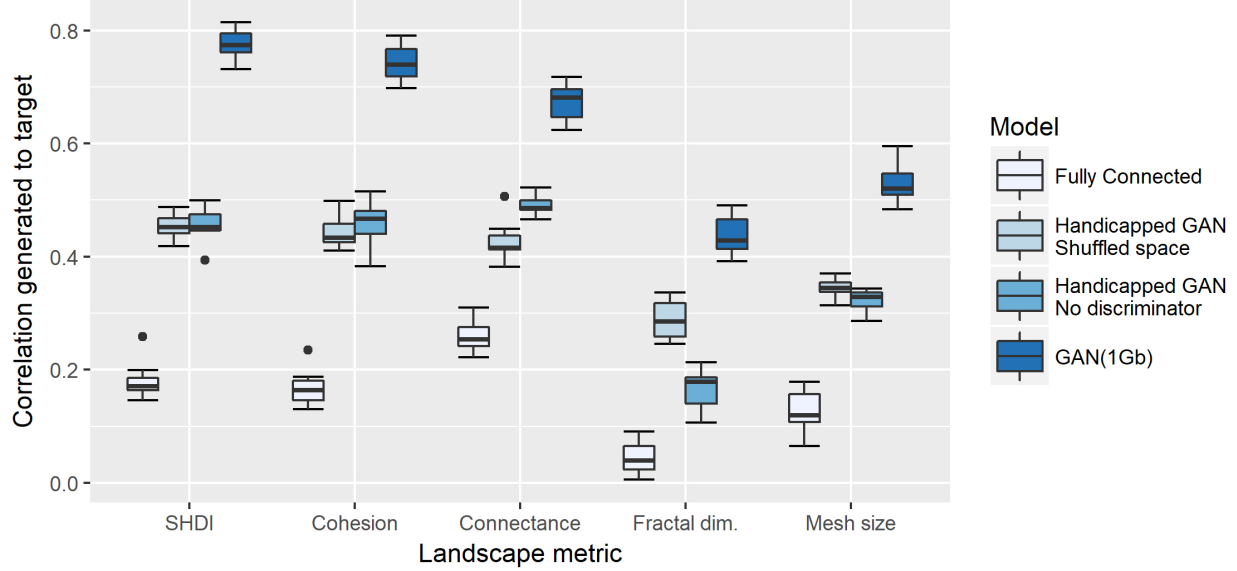


Figure 7: Intermodel comparison (8 landcover units) Robust biweight midcorrelation between landscape metrics of generated and target landscapes. Shannon diversity index (SHDI), patch cohesion, patch connectance, average patch fractal dimensionality and effective mesh size were computed for both, real landscapes of test locations, and landscapes generated given the environmental conditions on the test locations. Landscapes were segmented into 8 different patch types, serving as an undersegmentation case, i.e., the number of landcover units is excessively low.

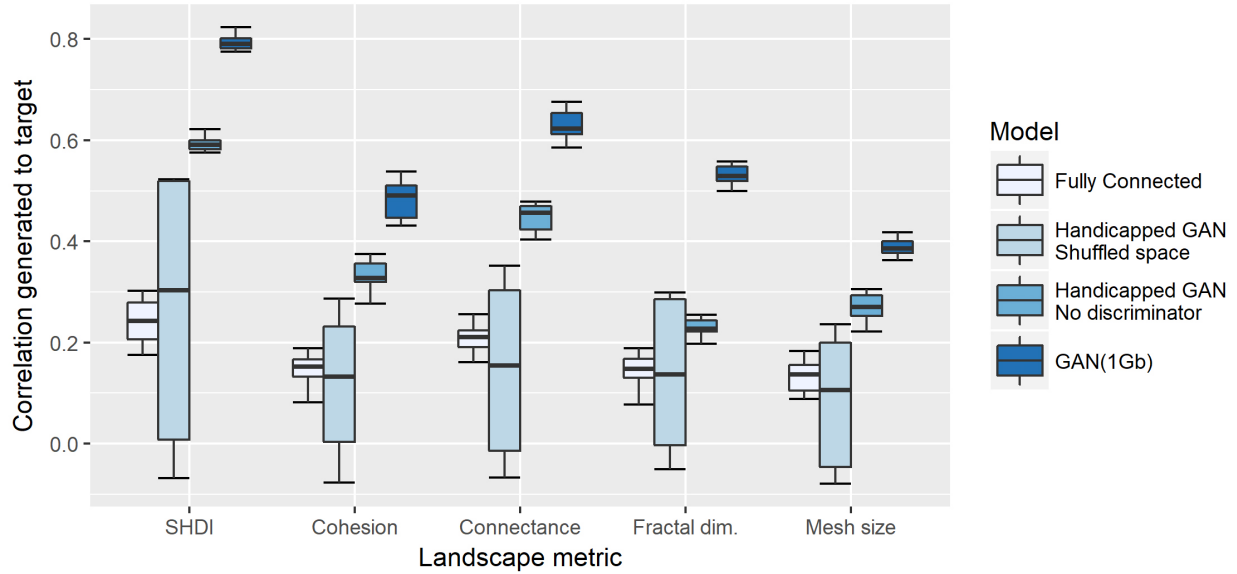


Figure 8: Intermodel comparison (60 landcover units) Robust biweight midcorrelation between landscape metrics of generated and target landscapes. Shannon diversity index (SHDI), patch cohesion, patch connectance, average patch fractal dimensionality and effective mesh size were computed for both, real landscapes of test locations, and landscapes generated given the environmental conditions on the test locations. Landscapes were segmented into 60 different patch types, serving as an oversegmentation case, i.e., the number of landcover units is excessively high.